30th International Conference
ENGINEERING MECHANICS 2024
Milovy, Czech Republic, May 14 – 16, 2024

ANALYTICAL INVESTIGATION OF MARS DRONE CONCEPTUAL DESIGN

Havran E.[*]

Abstract: *An analysis of Mars rotary wing aircraft was done, regarding a quadcopter design. A mission profile was proposed, that could be generalized to multiple mission goals. Energy requirements for such a mission were computed and then a mass sizing of the drone was calculated. This resulted in various design points of Mars drones, in accordance with what initial conditions (for example rotor count) were chosen. Next, using blade element momentum theory, an analytical model of the rotors was calculated and implemented to the drone, so as to create a conceptual design for later research and development use.*

Keywords: Mars drone, conceptual design, mass sizing, blade element momentum theory.

1. Introduction

As Mars exploration picks up its pace, with multiple planned missions in the next decades, the exploration and possible colonization of the planet will require more advanced technologies. A capability gap exists between immobile landers, mobile rovers that can nevertheless cover only a small distance in comparison with the surface of the planet and orbiting satellites that can cover large swaths of it at the expense of resolution of the pictures when dealing with surface mapping, or inability to take samples from interesting areas. Mars aircraft, especially ones with vertical take-off landing capabilities, offer a huge opportunity to bridge this gap, as was laid out by Young (2000). In recent years a technological demonstrator- the Ingenuity Mars Helicopter, was designed and tested on Mars, proving the applicability of rotary wing aircraft usage on the planet. However, Ingenuity only had a small size with no scientific payload and as such, larger Mars drones are being developed. While only in the conceptual phases, examples could include the work by NASA published for example in Johnson and Withrow-Maser (2020) or work by Aoki et al. (2018). Both used slightly different conceptual design principles to create the concept and as such there was slight variation of the results. For creating a new conceptual design of a Mars drone, utilizing both of these design processes and implementing knowledge of the blade element momentum theory of helicopters, a qualitative and quantitative analysis of a general Mars drone could have been created. The author utilized this as part of his diploma thesis (Havran, 2023).

Mars has a different environment than Earth. For rotary wing aircraft this is mainly noticeable in the very thin atmosphere, which also has a different composition. This results in a very low Reynolds number and Mach number of the flows, creating a specific case not encountered on Earth, explained by Koning et al. (2018). The decrease in rotor performance thanks to the thin atmosphere is alleviated a little by the lower gravitational acceleration on Mars.

2. Mission profile and energy requirement

Before a Mars drone could be designed, a mission profile needed to be created. A study by Balaram and Daubar (2019) listed possible mission goals. To design a concept, that can be utilized for multiple mission goals, considering a general mission profile without a specific mission goal was beneficial.

[*] Ing. Edmund Havran: Institute of Aerospace Engineering, Brno University of Technology, Technická 2896/2; 616 69, Brno; CZ, edmund.havran@vut.cz

doi: 10.21495/em2024-110

It consisted of the following parts: 1) Wake-up from sleep and preparation for flight; 2) Take-off; 3) Climb to altitude of 200 meters; 4) Flight for a distance of 1 000 meters with forward speed of 5 m/s; 5) Hovering for 2 minutes; 6) Descend to 0 meters; 7) Landing; 8) Recharge and sleep for 1 sol till the next mission. Energy requirements for one day of operations were calculated in accordance with Dorling et al. (2017) for the in-flight part. Landed energy consumption assumed a steady power usage of 10 W. Total energy required for the drone for 1 sol is shown in Fig. 1. in relationship with the assumed drone mass M_{total}.

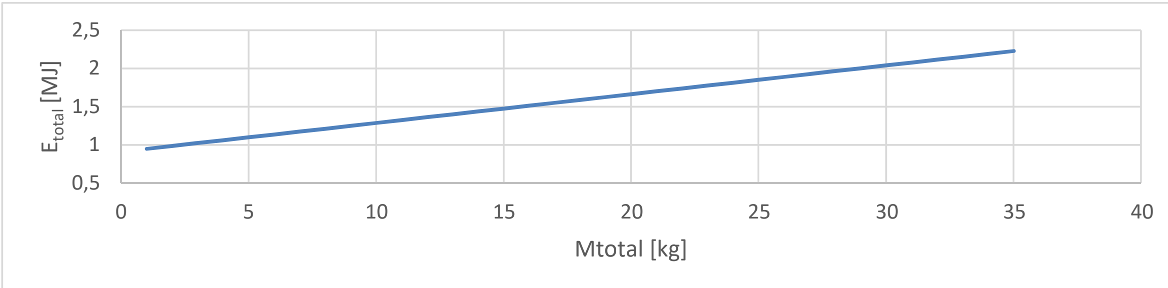

Fig. 1: Total energy required for 1 sol in relationship with total drone mass.

2.1. Mass sizing

Two methods for mass sizing were evaluated. Method 1 stemmed from Johnson (2020) and method 2 from Aoki et al. (2018). For the sake of brevity, only method 1 is described in this paper. Before both could be utilized, drone rotor disk count had to be decided. Four cases were studied: a tricopter, quadcopter, hexacopter and octacopter. A design assumption of variables is given in Tab. 1 approximated from other Mars drone concepts listed in Havran (2023). Drone masses from 1 to 35 kg were considered.

Coefficient of thrust	C_T	0.02	[-]
Coefficient of torque	C_Q	0.0023	[-]
Solidity	σ	0.18	[-]
Rotor tip speed	V_{tip}	0.7	Mach

Tab. 1: Assumed variables.

Rotor tip speed was limited to only 0.7 Mach to create a large cushion of possible improvement in forward speed and rotor performance in following studies and ensure appropriate results in the concept design phase. For method 1, total blade area A_b, masses of the blade, supporting arms from the fuselage to the rotor housing, fuselage, landing gear, motors and battery were first calculated. As these values used rotor radius and blade area, different results could have been achieved by having different rotor counts. For simplicity's sake, only the quadrotor was further analyzed.

$$A_b = \sigma \cdot A \tag{1}$$

$$M_{blade} = 1.1 \cdot A_b \tag{2}$$

$$M_{arm} = 0.2 \cdot r_{rotor} \tag{3}$$

$$M_{fuselage} = 28 \cdot \left(\frac{M_{total}}{1000}\right)^{\frac{2}{3}} \tag{4}$$

$$M_{gear} = 0.067 \cdot M_{total} \tag{5}$$

$$M_{motor} = \frac{P_{Fhove}}{\rho_{motor}} + M_{controller} \tag{6}$$

$$M_{bat} = \frac{1.3 \cdot E_{total}}{\rho_{bat}} \tag{7}$$

Controller mass was assumed to be 0.11 kg. Power density of the motor ρ_{motor} was chosen in accordance with off-the shelf components available for RC airplanes as 2 500 W/kg. Battery power density ρ_{bat} of 218.5 Wh/kg including the battery management system and assuming end of life cycle was chosen. This value was commercially available in high end products. To prolong the battery life, it was necessary to ensure energy reserves both on top and low ends of the battery charge. This was achieved by adding

30 % to the total required energy. Recharging the battery was done by solar panels. Their size depended on recharge time and rate, so a total time in direct sunlight during 1 sol was calculated as 35 % of a sol, about 5.6 hours. From this the needed charging power of the solar panels was calculated.

$$P_{solar} = \frac{E_{total}}{0.35 \cdot t_{sol}} \tag{8}$$

Taking the values introduced in Johnson (2020) for solar cell power density of 21.9 W/m^2 and mass density of 2 kg/m^2 allowed solar cell mass to be calculated.

$$M_{solar} = 2 \cdot A_{solar} \tag{9}$$

Two additional constant masses added were for avionics at 1.2 kg, including navigational and communicational equipment and a payload reserve of 2.02 kg without specification. The total mass M_{total} was first assumed to the values of 1 to 35 kg.

Results are shown in Fig. 2. These also included a version with 15 % added mass as a buffer, because it could be expected that empirical formulas used for mass assumption were not accurate. Msum corresponds to the mass calculated from above formulas. Mass divergence shows the difference between the calculated M_{total} and initially assumed M_{total}. If the initially assumed mass and calculated one are the same – the divergence is 0- then a design point was formed. Changing the required payload, or flight profile changed the design point too and thus a large array of values could have been quickly evaluated.

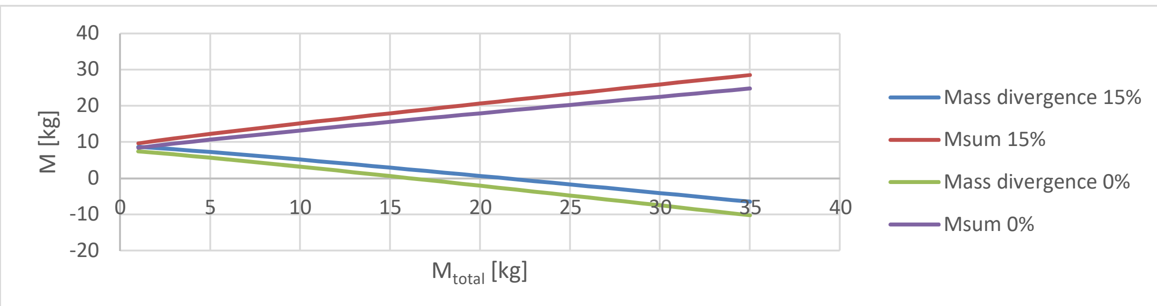

Fig. 2: Mass convergence graph.

2.2. Aerodynamics of rotors

Aerodynamic analysis using blade element momentum theory (BEMT) was utilized. The principle of BEMT was that a nondimensional rotor induced inflow ratio λ in hover could be computed, assuming a linear lift polar curve shape of an airfoil. A known and tested triangle airfoil by Suwa et al. (2012) was assumed, where a clearly linear part of its lift polar was narrowed down. The blade was also assumed to be of rectangular planform and with constant pitch angle along its span. The calculations used by BEMT were widely published, for example in Leishman (2008).

Flow around the rotor blade was influenced by induced flow and this resulted in different real angles of attack of the flow on the blade. Thanks to the induced inflow ratio, the final effective angle of attack α along the blade was calculated from the pitch angle of the blade (a given geometrical property of the blade). Fig. 3 shows the effective angle of attack along the blade radius r for different pitch angles of the blade. This was shown for a drone mass of 15 kg. Fig. 4 on the other hand shows the effective angle of attack for pitch angle of 2 ° for various drone design points.

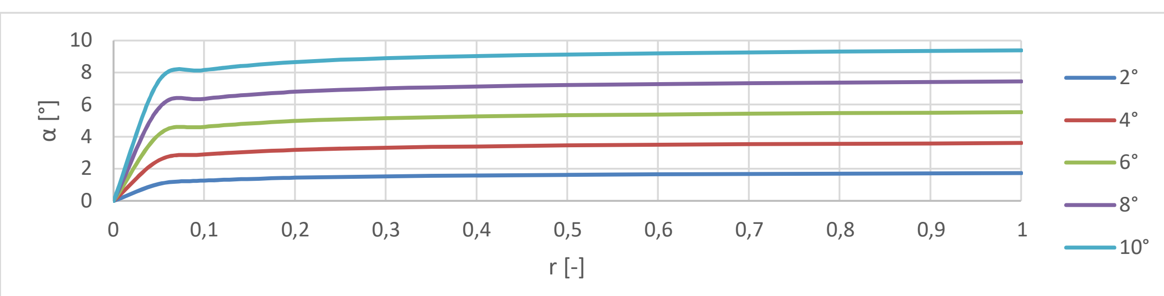

Fig. 3: Effective angle of attack for different pitch angles for a drone with a mass of 15 kg.

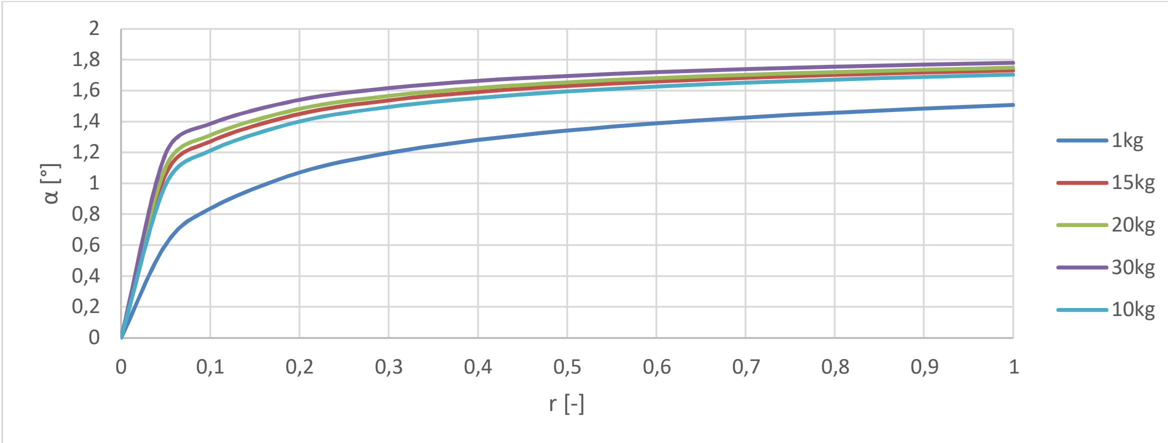

Fig. 4: Effective angle of attack for different drone masses for a blade pitch angle of 2 °.

3. Conclusions

Utilizing aerodynamic characteristics of the rotors, drone mass and a components list, a finalized conceptual design of the drone was created. As the used airfoil was not optimized and the blade was assumed to be of rectangular shape, the resulting drone performance could be vastly improved upon by a specifically designed and optimized rotor blade using better airfoils. As such, the resulting graphs useful for the conceptual design phase of a Mars multicopter and could be used with little modifications to provide a base for more advanced and specific research and development of a Mars rotary wing vehicle in multiple possible configurations and mission goals.

Acknowledgement

This work has been supported by the project No. FSI-S-23-8163 funded by The Ministry of Education, Youth and Sport (MEYS, MŠMT in Czech) institutional support.

References

Aoki, R. et al. (2018) Conceptual Helicopter Design for Exploration of Pit Craters and Caves on Mars, In: *AIAA Atmospheric Flight Mechanics Conference*, AIAA SPACE Forum, Orlando, FL.

Balaram, J. et al. (2019) Helicopters on Mars: Compelling Science of Extreme Terrains Enabled by an Aerial Platform, *9th International Conference on Mars*, Pasadena, 6277.

Dorling, K., Heinrichs, J., Messier, G.G. and Magierowski, S. (2017) Vehicle Routing Problems for Drone Delivery, *IEEE Transactions on Systems, Man, and Cybernetics: Systems*, 47(1), pp. 70–85.

Havran, E. (2023) *Mars Drone conceptual design*. Diploma thesis, Brno University of Technology, Faculty of Mechanical Engineering, Institute of Aerospace Engineering.

Johnson, W. and Withrow-Maser, S. (2020) *Mars Science Helicopter Conceptual Design*. Moffet Field, CA, Ames Research Center.

Koning, W. J. F., Allan, B. G. and Johnson W. (2018) Generation of Mars Helicopter Rotor Model for Comprehensive Analyses, In: *AHS Specialists´ Conference on Aeromechanics Designs for Transformative Vertical Flight*, San Francisco, CA, 22 p.

Leishman, J. G. (2008) *Principles of helicopter aerodynamics*. 2nd edition, Cambridge University Press, Aerospace Series, Cambridge.

Suwa, T., Nose, K., Numata, D., Nagai, H. and Asai, K. (2012) Compressibility Effects on Airfoil Aerodynamics at Low Reynolds Number, In: *30th AIAA Applied Aerodynamics Conference*, AIAA, Reston, VA.

Young, L. A. (2000) *Vertical Lift – Not Just For Terrestrial Flight*. Moffet Field, CA, Ames Research Center.